

The Effect of CO₂ Pressure on Chromia Scale Microstructure at 750°C

B.A. PINT^{1,2} and K.A. UNOCIC¹

1.—Oak Ridge National Laboratory, P.O. Box 2008, Oak Ridge, TN 37831-6156, USA. 2.—e-mail: pintba@ornl.gov

To understand and model performance in supercritical CO₂ (sCO₂) for high-efficiency, concentrating solar power (CSP) and fossil energy power cycles, reaction rates are compared at 750°C in 0.1 MPa CO₂ and 30 MPa sCO₂ as well as laboratory air as a baseline on structural materials such as Ni-based alloy 625. Due to the thin reaction products formed even after 5000 h, scanning transmission electron microscopy was used to study the Cr-rich surface oxide scale. The scales formed in CO₂ and sCO₂ had a much finer grain size with more voids observed in CO₂. However, the observations on alloy 625 were complicated by Mo and Nb-rich precipitates in the adjacent substrate and Al internal oxidation. To simplify the system, a binary Ni-22Cr alloy was exposed for 1000 h in similar environments. After exposure in sCO₂, there was an indication of carbon segregation detected on the Cr₂O₃ grain boundaries. After exposure in air, metallic Ni precipitates were observed in the scale that were not observed in the scale formed on alloy 625. The scale formed in air on a second Ni-22Cr model alloy with Mn and Si additions did not contain Ni precipitates, suggesting caution when drawing conclusions from model alloys.

INTRODUCTION

The interest in compatibility of structural alloys with supercritical CO₂ (sCO₂) for nuclear, solar and fossil energy applications^{1–4} has renewed the question about the role of pressure in high-temperature degradation.^{5–8} An ongoing project is generating longer-term data at 700–800°C to model lifetime.^{9,10} For example, a 30-year lifetime for a concentrating solar power (CSP) application will require more than 100,000 h of hot time. Temperatures over 700°C are required to achieve > 50% efficiency in the power block.¹¹ The oxygen partial pressure in CO₂ is similar to that in steam;⁸ thus, typical oxides are able to form on conventional Fe- and Ni-based alloys. Based on the considerable research associated with the development of the United Kingdom gas cooled nuclear reactors,^{12–17} the most significant concern with CO₂ environments is internal carburization,¹⁸ particularly for Fe-based alloys.^{12,13,17–21}

Above 700°C, Ni-based alloys are needed because of their higher strength,²² typically, such alloys have 16–25% Cr and reasonably good oxidation resistance due to the formation of a Cr-rich reaction product^{23–28} including in sCO₂.^{7–10,21,29–31}

Previously, mass change data at 750°C in 30 MPa sCO₂ were reported⁹ and the oxide-scale microstructure investigated using scanning transmission electron microscopy (STEM) after 1000 h of exposure.¹⁰ Because of the thin but complicated reaction products on precipitation strengthened (PS)²² Ni-based alloys, the current work examined scale microstructures after 5000-h exposures on solid solution (SS) strengthened alloy 625 to understand the evolution of the scale at longer exposure times in laboratory air and 0.1 MPa CO₂ and 30 MPa sCO₂. To further understand the effect of environment on the scale microstructure without the complication of the strengthening additions, model Ni-22Cr alloys also were examined.

EXPERIMENTAL PROCEDURE

Coupons (~ 10 × 20 × 1.5 mm) with a 600-grit finish were cut from a commercial heat of alloy 625 (60.6 wt.% Ni-21.7Cr-9.4Mo-4.0Fe-3.6Nb-0.2Ti-0.2Si-0.1Mn-0.1Co-0.09Al-0.016C) and laboratory cast and hot-rolled model Ni-21.9Cr and Ni-21.2Cr-1.4Mn-0.5Si alloys. Prior to oxidation, 6–10 alloy 625 coupons per condition were ultrasonically

cleaned in acetone and methanol, and all exposures used 500-h cycles with specimens cooled and weighed between each cycle. For exposures in laboratory air, the coupons were placed in an alumina holder in an alumina boat and heated in a box furnace (no gas flow) for ~ 4 h to 750°C , held for 500 h and cooled slowly. For exposure in 0.1 MPa, industrial-grade (IG) CO_2 , with < 50 ppm O_2 and 18 ± 16 ppm H_2O , the coupons were placed in alumina boats in an alumina reaction tube with

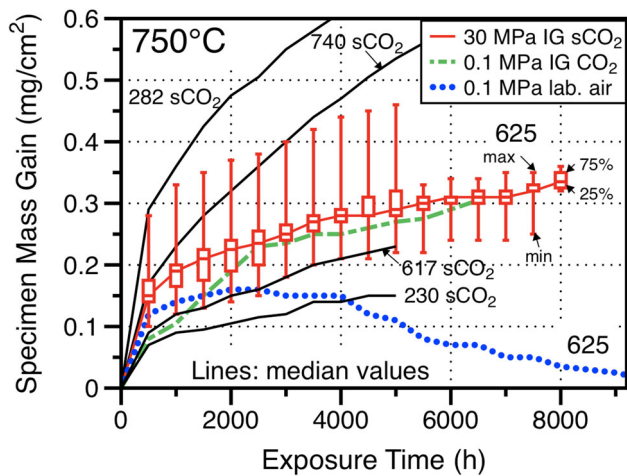


Fig. 1. Specimen mass gain at 750°C in 500-h cycles for alloy 625 in three different environments. The lines show median values for 6-10 specimens in each condition. The box and whiskers show the distribution of values at each measurement in 30 MPa IG sCO_2 . For comparison, median values in 30 MPa IG sCO_2 for four other Ni-based alloys are shown.

end caps. The specimens were heated in flowing Ar to 750°C over 4 h, held for 500 h in IG CO_2 and cooled in flowing Ar to room temperature. Gas flow rates were ~ 300 ml/min or ~ 0.1 cm/s flow rate. For the 500-h cycles in 30 MPa IG sCO_2 , the experiments were conducted in an autoclave fabricated from alloy 282³² with the specimens suspended on alumina rods with alumina spacers between specimens.⁷ The fluid flow rate was ~ 2 – 3 ml/min. The autoclave was slowly heated to temperature over several hours ($\sim 2^\circ\text{C}/\text{min}$) in sCO_2 , held at temperature $\pm 2^\circ\text{C}$ and then cooled in sCO_2 to room temperature by lowering the furnace and using a cooling fan on the autoclave.

Specimen mass change was measured every 500-h cycle using a Mettler Toledo XP205 balance with an accuracy of $\sim \pm 0.04$ mg or 0.01 mg/cm². The specimens for STEM analysis were prepared via the in situ lift-out method using focused ion beam (FIB) milling on a Hitachi NB5000 FIB-SEM. A W layer was deposited to protect the gas interface of the scale. The STEM imaging was carried out using a FEI model Talos F200X STEM with an integrated energy dispersive x-ray spectrometer (EDS) with four silicon drift detectors.

RESULTS

Figure 1 shows the specimen mass change data for the alloy 625 specimens in three different environments. The dashed and solid lines denote the median values of 6-10 specimens in each environment. The box and whisker plots indicate the range of values measured in 30 MPa IG sCO_2 and indicate scatter in the transient stage of

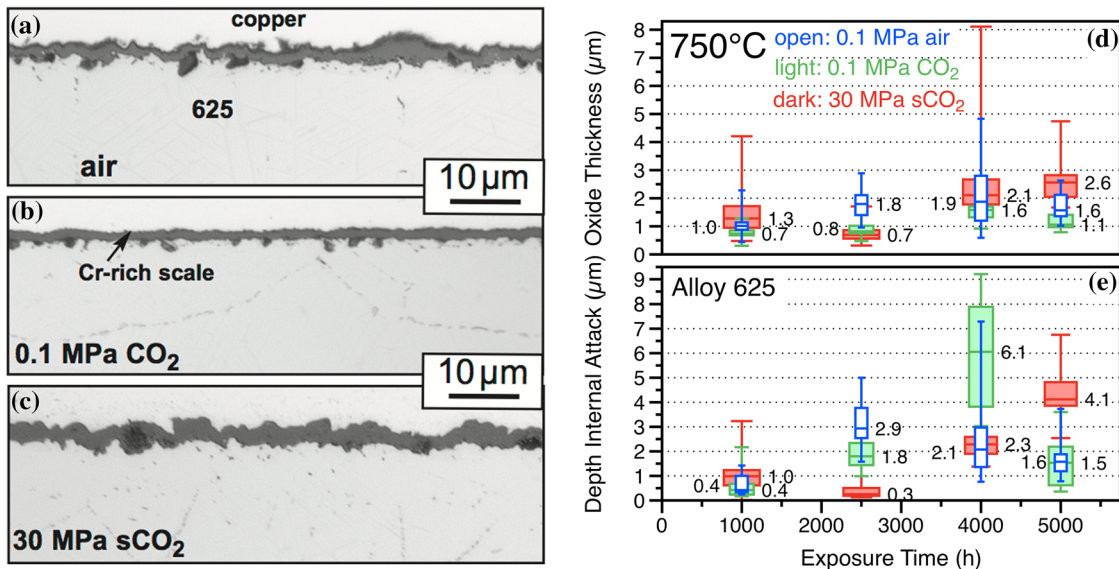


Fig. 2. Light microscopy of alloy 625 specimens exposed for 5000 h in (a) laboratory air, (b) 0.1 MPa IG CO_2 , (c) 30 MPa IG sCO_2 and measurements versus exposure time for alloy 625 specimens (d) scale thickness and (e) depth of internal oxidation. The box and whisker plots show the minimum and maximum values measured (~ 30), and the box is defined by the 25% and 75% values with the median value noted

oxidation. The boxes are not shown for the other conditions for clarity. Median values for several other SS (alloys 230 and 617) and PS (alloys 282 and 740) Ni-based alloys in 30 MPa IG sCO₂ are shown for comparison. The PS alloys have higher mass gains due to the internal oxidation of Al and Ti in these alloys.^{7–10} The median mass change in 0.1 MPa IG CO₂ was remarkably similar to the values at 30 MPa and suggests a limited effect of CO₂ pressure on the reaction, in agreement with prior work at 12–30 MPa for 500 h.⁸ In laboratory air, the mass gain was initially similar after the first cycle but, at longer times, the mass dropped and then followed a very slow decline in mass. Rather than spallation, which was not observed, Mo (or Cr) evaporation is suspected.

Figure 2a, b and c shows representative light microscopy of polished scale cross-sections formed on alloy 625 at 750°C after 5000 h exposures in each environment. The oxides show some variation in thickness but are all relatively thin, consistent with the mass change data in Fig. 1. Figure 2d shows measurements of the oxide thickness in the three environments as a function of exposure time (4 different specimens were removed from the experiment at intervals and sectioned). Likewise, in Fig. 2e, the depth of internal oxidation was quantified. Consistent with the similar mass change data, the oxides are similar in thickness with a limited amount of internal oxidation. Even after 5000 h exposures, the scales were thin and required higher resolution characterization to detect changes in the microstructure.

Figure 3 shows bright-field (BF)-STEM images of the scale cross-sections after 5000 h exposures that were shown in Fig. 2. The grains appear to be larger in the scale formed in air (Fig. 3a) and finest in the scale formed in 0.1 MPa CO₂ (Fig. 3b). In the area sectioned, the scale formed in 30 MPa sCO₂ appears slightly thicker, consistent with the measurements in Fig. 2d. Again, judging by the area sectioned in Fig. 3b and c, the porosity in the scale and at the metal-scale interface appeared to be higher after exposure at 0.1 MPa CO₂. Figure 4 shows EDS elemental maps of the images in Fig. 3. As expected, the scales are mainly Cr₂O₃ and contain a uniform low level of Mn with minor Ti incorporation. The low level of Al in the alloy forms internal oxides in each case. To complicate the analysis, Mo and Nb form precipitates at the metal-scale interface as they are rejected from the reaction front.³³ As noted for the analysis of scales formed after 1000 h,¹⁰ some C could be detected in each of the scales but there did not appear to be any enrichment of C in the scale or adjacent substrate. Sputter depth profiles using glow discharge optical emission spectroscopy (GDOES) also did not detect any C enrichment after exposure of

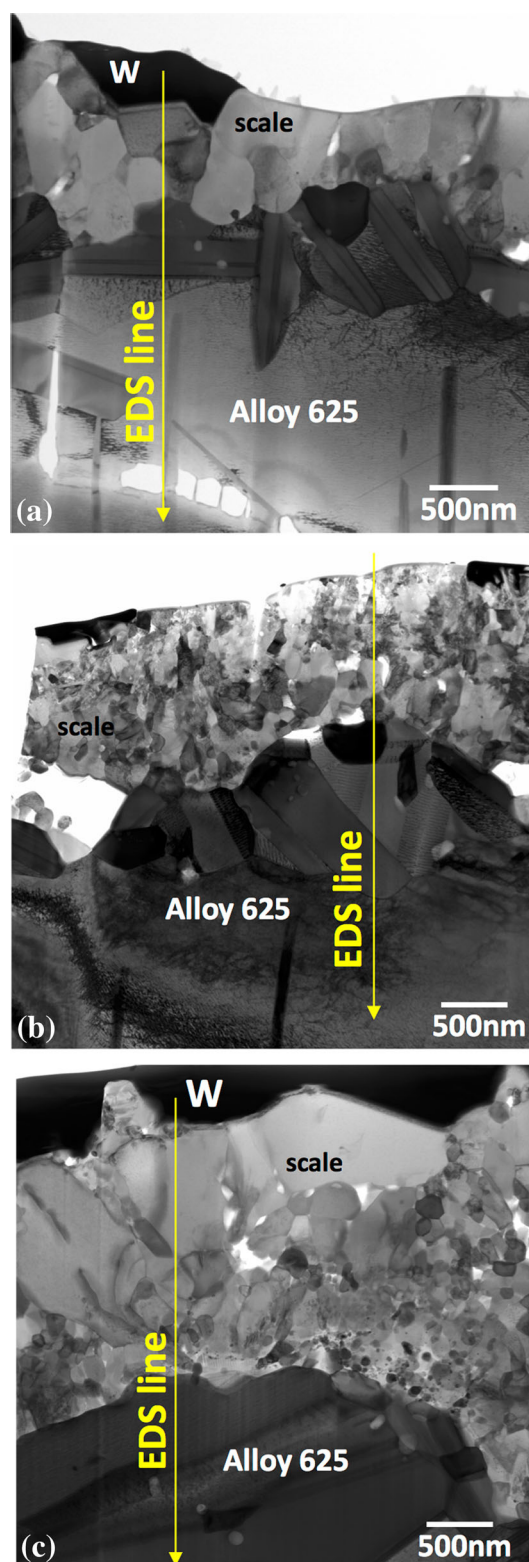


Fig. 3. BF-STEM cross-sectional images of the scales formed on alloy 625 after 5000 h exposures at 750°C in (a) laboratory air, (b) 0.1 MPa CO₂, and (c) 30 MPa sCO₂.

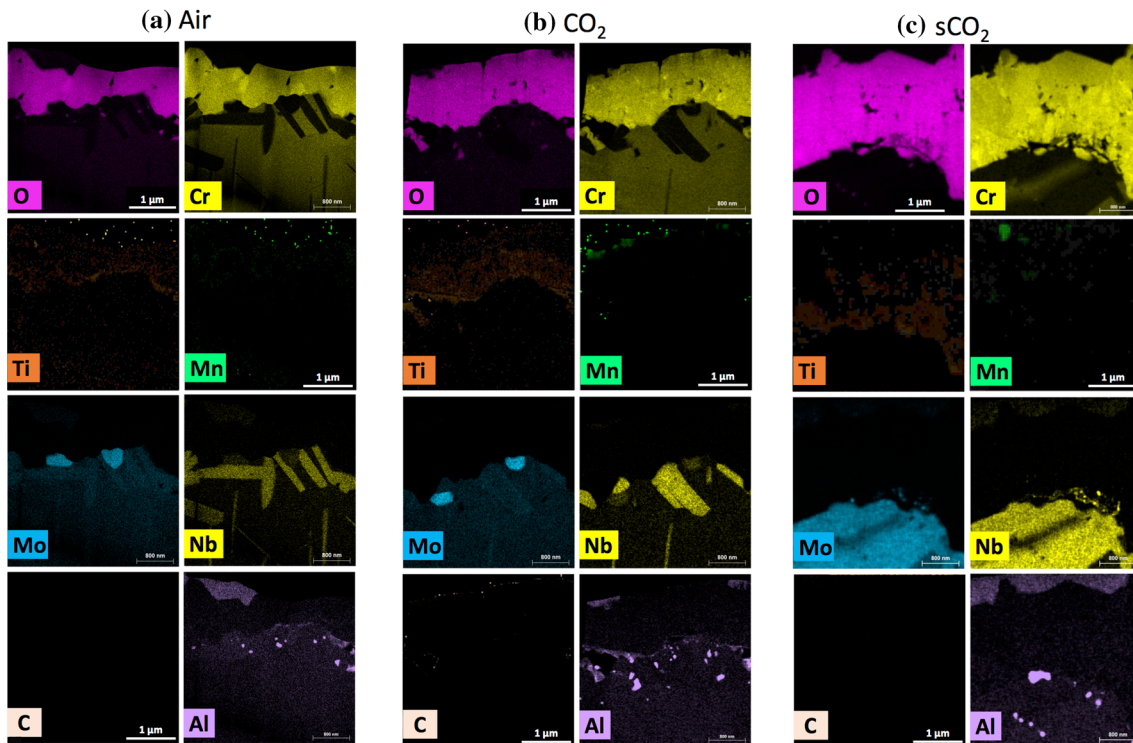


Fig. 4. EDS elemental maps associated with the images in Fig. 3 of scales formed on alloy 625 after 5000 h exposures at 750°C in (a) laboratory air, (b) 0.1 MPa CO₂, and (c) 30 MPa sCO₂.

this specimen.³⁴ EDS line profiles in Fig. 5 are from lines marked in Fig. 3. Again, the scale is primarily Cr₂O₃, and the Mo- and Nb-rich precipitates stand out in the substrate adjacent to the scale. Very low levels of Mn and Ti were detected in the scale.

To better understand the role of the environment on Cr₂O₃ formation without the complications of internal oxidation and alloy precipitates, model Ni-22Cr alloy specimens were exposed for 1000 h (2 cycles) in air and 30 MPa sCO₂. The reaction products are shown in Fig. 6. Similar to alloy 625, much larger Cr₂O₃ grains were observed to form in air. For the scale formed in air, Ni-rich metallic precipitates could be seen near the metal-scale interface at higher magnification (Fig. 7). Similar metal precipitates were observed in the scale formed on Fe–Cr alloys in air or steam at 1200°C³⁵ and were hypothesized to form in many scales.³⁶ Interestingly, similar Ni-rich precipitates did not form during exposure in 30 MPa sCO₂. On further analysis of the scale formed in sCO₂, C could be detected weakly segregated to the oxide scale grain boundaries, as shown in two EDS line profiles in Fig. 8. This is similar to the observation of grain boundary C segregation using atom probe tomography of the Cr₂O₃ scale formed on Fe-20Cr exposed to Ar-20CO₂ for 120 h at 650°C.³⁷

One final experiment was conducted on a model Ni–Cr specimen that also contained Mn and Si additions. Figure 9 shows the thicker scale formed in air on this alloy after 1000 h (2 cycles), where the outer layer of the scale is a mixed Cr and Mn oxide. The Si addition results in a non-uniform, amorphous SiO₂ layer at the metal-scale interface. However, the most interesting feature is that no Ni-rich precipitates were observed in the scale formed on this alloy (Fig. 10). This is similar to observations for Fe–Cr model alloys oxidized in air and steam at 1200°C where no Fe precipitates were observed in the scale formed on Fe-22Cr + Mn, Si.³⁵

DISCUSSION

The results in Figs. 1 and 2 suggest that the compatibility of Ni-based alloys like 625 is not a concern in an sCO₂ environment with relatively high purity IG CO₂ and is not significantly different from oxidation in laboratory air. Although in air the slight mass loss without obvious scale spallation suggests evaporation may be occurring, this mechanism requires further study to confirm if Mo was evaporating. Furthermore, the 30 MPa pressure and supercritical state of CO₂ appeared to have

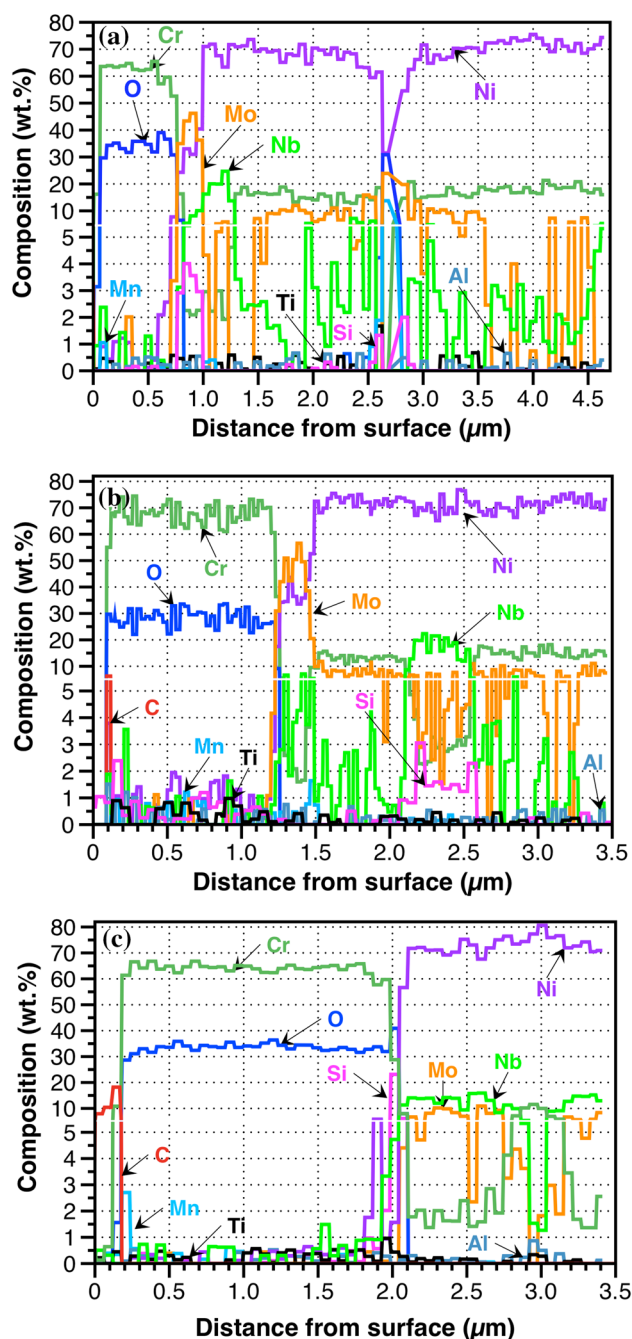


Fig. 5. EDS line profiles associated with the images in Fig. 3 of scales formed on alloy 625 after 5000 h exposures at 750°C in (a) laboratory air, (b) 0.1 MPa CO₂, and (c) 30 MPa sCO₂.

little effect on the reaction, although the scale thickness was slightly higher compared with the exposures at 0.1 MPa in CO₂ and laboratory air. No evidence of internal carburization was observed under these conditions. The lack of a pressure effect

suggests that results obtained at 0.1 MPa or even 4.3 MPa for the UK gas-cooled reactors^{14–17} may be applicable to predicting behavior under sCO₂ conditions. A similar conclusion was reached after 500-h exposures at 12–30 MPa.⁸

The STEM analysis of the relatively thin scale cross-sections formed after 5000 h clearly showed that the grain size was finer when formed in CO₂ or sCO₂. Compared with the prior observations for alloy 625 after 1000 h,¹⁰ the scale continued to thicken by nucleating additional grains. The finer grains could suggest the presence of a segregant that inhibited grain growth, but no C or other species was detected for the scales formed in 0.1 MPa CO₂ or 30 MPa sCO₂ on 625 specimens. Carbon segregation was detected in scale grain boundaries formed on binary Ni-22Cr, similar to prior observations for scales formed on Fe-20Cr.³⁷ Previously, it was concluded that C had no significant solubility in Cr₂O₃.³⁸ However, those experiments were conducted on bulk ceramics exposed to CO-CO₂ where there was no active oxidation reaction occurring.

Because of the presumed lack of solubility, it is often assumed that C ingress occurs via cracks, pores and possibly grain boundaries³⁷ in the scale. The scales observed here did not contain obvious defects besides some porosity, which may explain the limited C ingress observed for these materials. (An alternative explanation is that Ni-based alloys are less susceptible to C ingress because of their lower C solubility compared with Fe-based alloys.²¹) The porosity appeared to decrease for the scale formed in sCO₂, perhaps because of an effect of the higher gas pressure. An alternative explanation for the fine grain size is that cracks or other defects may fill with new fine grains or that the presence of C assists in the nucleation of new oxide grains (rather than inhibiting growth). Note that it is difficult to draw conclusions about the scale microstructure because of the limited areas sectioned for STEM analysis.

After 1000 h exposures, model alloys were studied to provide less complicated microstructures for analysis. Similar to the observations for alloy 625, Fig. 6 indicates that the scale formed in sCO₂ had a smaller grain size than the scale formed in air, although the oxide grains were not as fine on the model alloy as on 625. However, some of the other observations, such as C segregation in sCO₂ and metallic Ni precipitates in air, were not observed in the scale on alloy 625 after 1000 h¹⁰ or 5000 h. The C segregation detected was very weak, barely above background. Previous work on scales formed on an advanced austenitic steel in air and sCO₂ at 700°C detected C in both environments,¹⁰ and it was concluded that STEM/EDS was not as effective as

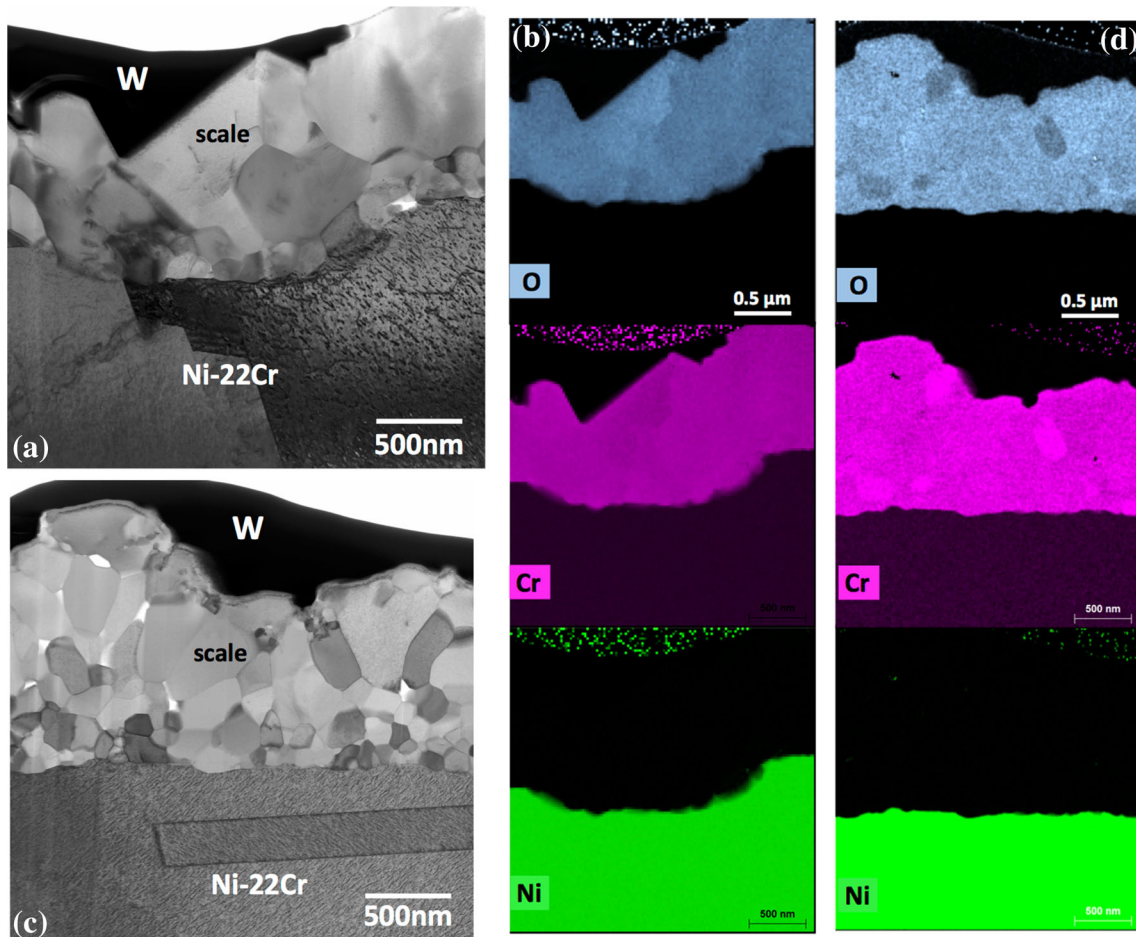


Fig. 6. BF-STEM cross-sectional images (a, c) and associated EDS elemental maps (b, d) of the scales formed on Ni-22Cr after 1000 h exposures at 750°C in (a, b) laboratory air and (c, d) 30 MPa sCO₂.

APT for this type of characterization when carbon is present at very low levels. No C segregation was detected in the scales formed on 625 specimens, only for the binary NiCr specimen, which is analogous to the APT results for C segregation in binary Fe-20Cr.³⁷

Since an addition like Mn inhibits carburization of Fe-20Cr in Ar-20%CO₂,³⁹ it would be interesting to understand if conventional steel additions such as Mo, Mn and Si also inhibit C segregation.

Finally, regarding the metallic Ni precipitates observed in the scale formed on Ni-22Cr in air, the first point is that they were not observed in the scale formed in sCO₂, perhaps because of the lower O₂ partial pressure in sCO₂. However, similar Fe precipitates were observed in prior work on Fe-Cr alloys oxidized in 0.1 MPa steam and air at

1200°C.³⁵ With the additions of Mn and Si in a second model Ni-Cr alloy, no Ni precipitates were observed in the Cr₂O₃ scale formed in air for 1000 h. It is not surprising that the precipitates appear to be metallic because the oxygen partial pressure in the scale near the interface should be near the Cr/Cr₂O₃ equilibrium and well below where NiO is stable. However, it is surprising that such a large amount of Ni was incorporated into the scale. The growth mechanism of Cr₂O₃ has not been studied at 750°C, but prior work on Ni-25Cr at 1000°C indicated mixed Cr and O transport.⁴⁰ Thus, the scale formed adjacent to the Ni-22Cr substrate likely formed by inward growth of O. On the binary alloy, Ni may have been incorporated, perhaps because of Cr depletion in the adjacent substrate. In the other alloys, a barrier effect of SiO₂ formation could

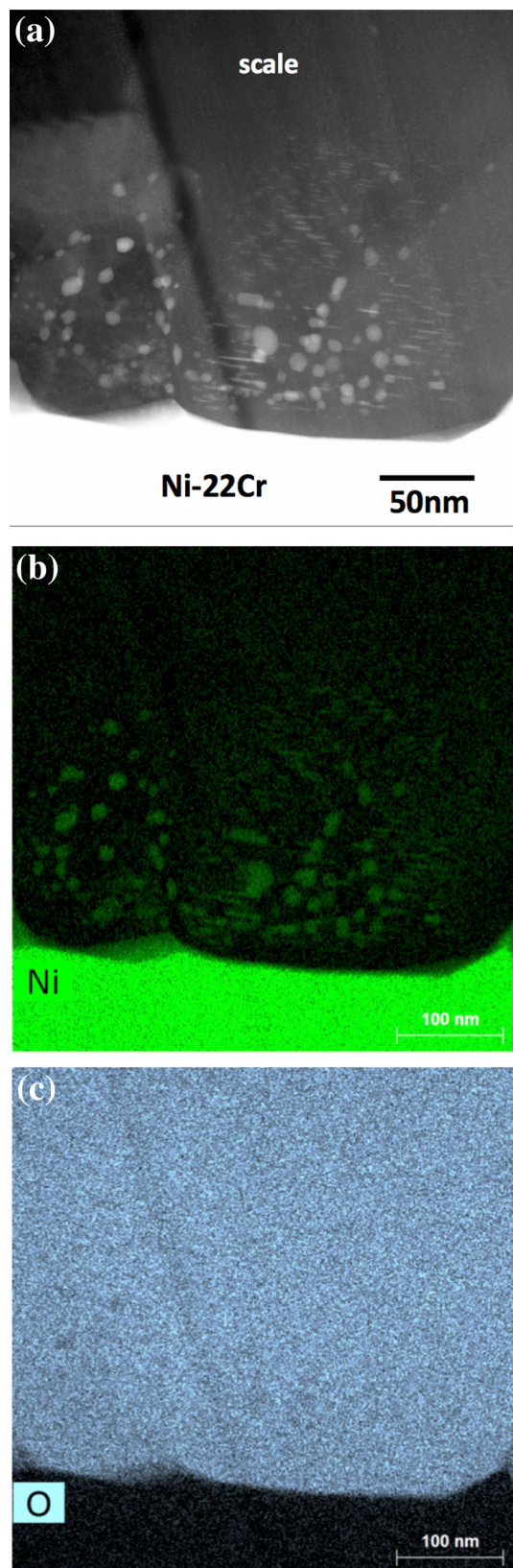


Fig. 7. (a) HAADF-STEM cross-sectional image near the metal-scale interface of Ni-22Cr after 1000 h at 750°C in air and EDS maps from (a): (b) Ni and (c) O.

inhibit Ni incorporation or the outward transport of Mn may have affected this behavior. Because the model alloy had higher levels of Mn (1.4 versus 0.1) and Si (0.5 versus 0.2) than alloy 625, it formed a more distinctive (but not continuous) layer of SiO₂ and a continuous outer layer rich in Mn (Fig. 9). The EDS elemental maps (Fig. 4) and line profiles (Fig. 5) suggest that Mn was incorporated into the scale formed on 625 but a Mn-rich layer did not appear to form, possibly because of the low level of Mn in the alloy. Thus, while model alloys may provide mechanistic insight, the results should be compared with commercial alloys to verify their relevance.

SUMMARY

The thin reaction products on alloy 625 were characterized using scanning transmission electron microscopy as a representative structure alloy for supercritical CO₂ (sCO₂) power generation applications. After 5000-h exposures at 750°C, the Cr₂O₃ grain size was smaller when formed in 0.1 MPa CO₂ or 30 MPa sCO₂ compared with the scale formed in laboratory air. However, the oxide scale formed in 30 MPa sCO₂ was thicker and contained fewer voids. In all cases, Al internal oxidation was observed along with the formation of Mo- and Nb-rich precipitates in the alloy 625 substrate adjacent to the scale. The scale formed on a binary Ni-22Cr substrate in 30 MPa sCO₂ after 1000 h also showed a finer grain size compared with a similar exposure in laboratory air. Carbon was found to segregate to grain boundaries in the sCO₂-formed scale. The scale formed in air contained Ni metallic precipitates near the metal-scale interface, but similar precipitates did not form in sCO₂ or in the scale formed in air on Ni-22Cr with Mn and Si additions.

In this case, several unique results found for the scales formed on binary Ni-22Cr may not be relevant to the objective of modeling long-term commercial alloy performance.

ACKNOWLEDGEMENTS

The author would like to thank M. Howell, M. Stephens, G. Garner, T. Lowe, T. Jordan, D. Coffey and C. Parrish at ORNL for assistance with the experimental work and S. Dryepondt and L. Allard for comments on the manuscript. The authors appreciate the donation of alloy 625 from Haynes International. This research was funded by the US Department of Energy's Office of Energy Efficiency and Renewable Energy, Solar Energy Technology Office: SuNLaMP award number DE-EE0001556 and by the Office of Fossil Energy (Grant No. FEAA123), Crosscutting Technology Program. The STEM work was supported by the Office of Nuclear Energy, Fuel Cycle R&D Program and the Nuclear Science User Facilities.

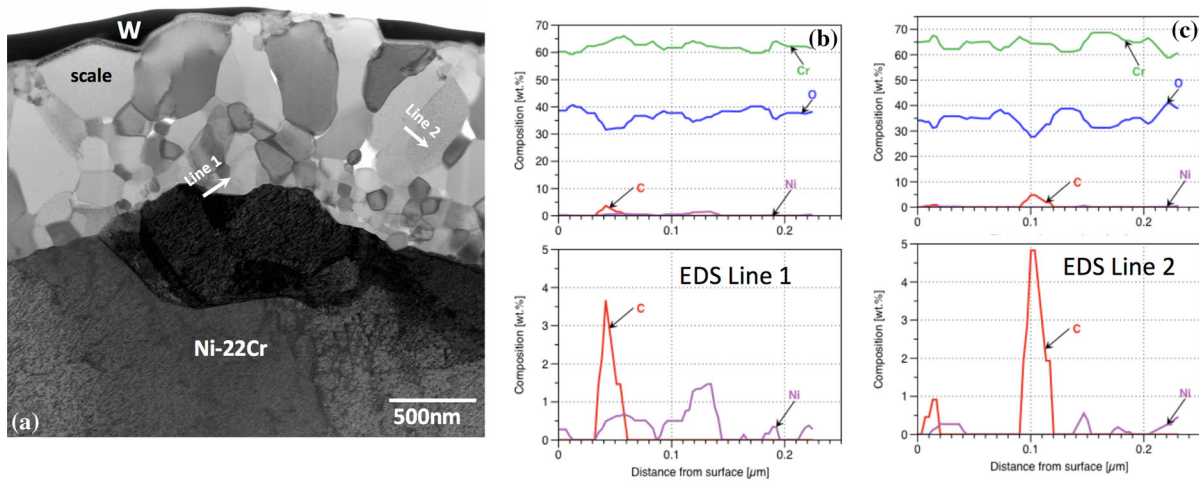


Fig. 8. (a) BF-STEM cross-sectional image of scale formed on Ni-22Cr after 1000 h at 750°C in 30 MPa sCO₂; location of line profiles in (b) and (c) are shown in (a).

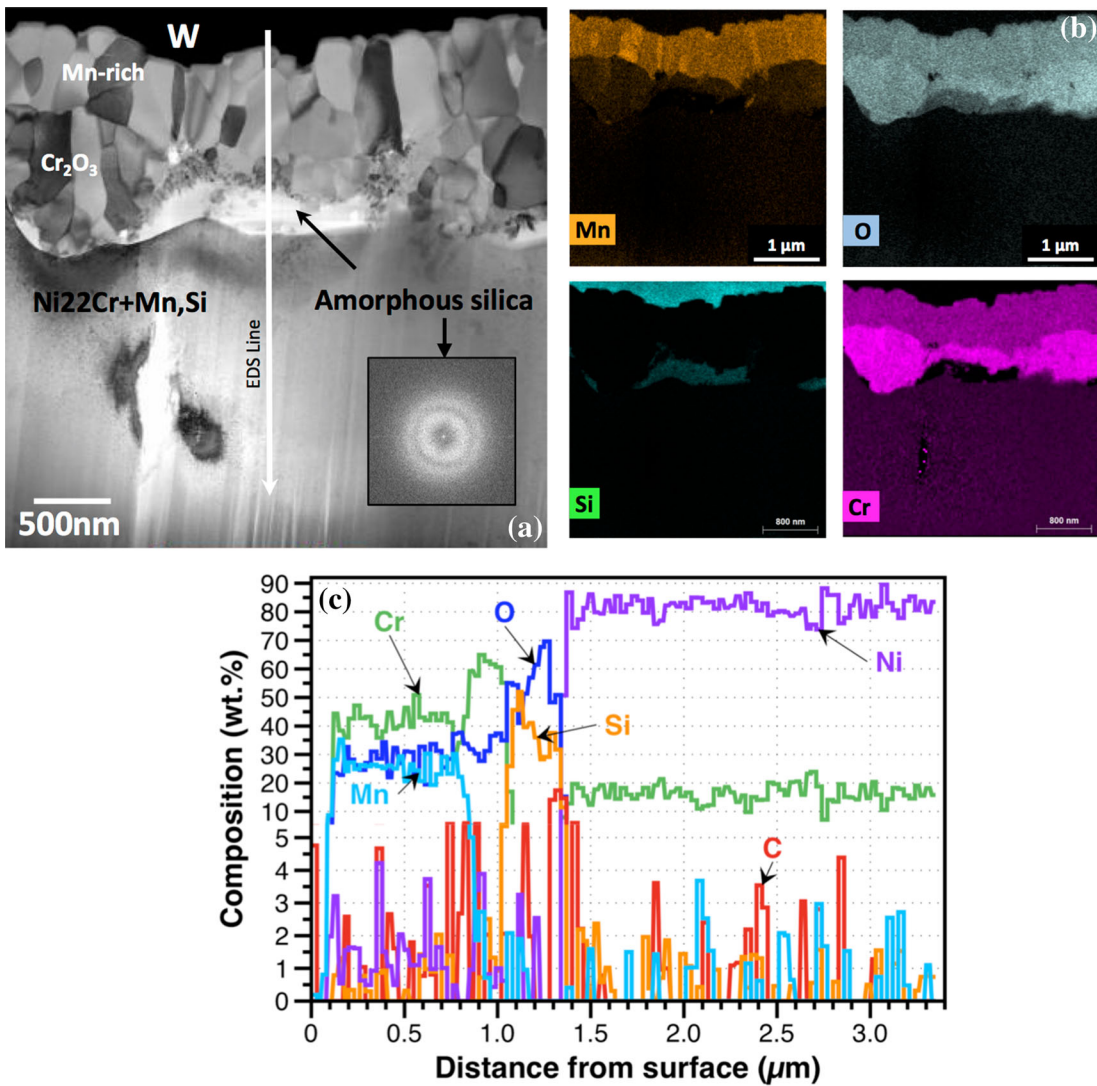


Fig. 9. (a) BF-STEM cross-sectional image of scale formed on Ni-22Cr + Mn,Si after 1000 h at 750°C in air. (b) EDX maps from (a). (c) Line profile through the scale in (a).

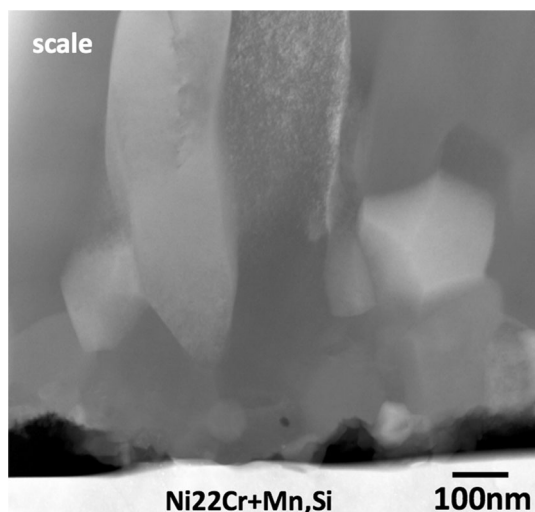


Fig. 10. HAADF-STEM cross-sectional image near the metal-scale interface of Ni-22Cr + Mn,Si after 1000 h at 750°C in air.

REFERENCES

- V. Dostal, P. Hejzlar, and M.J. Driscoll, *Nucl. Technol.* 154, 265 (2006).
- B.D. Iverson, T.M. Conboy, J.J. Pasch, and A.M. Krui-zenga, *Appl. Energy* 111, 957 (2013).
- R.J. Allam, M.R. Palmer, G.W. Brown Jr, J. Fetvedt, D. Freed, H. Nomoto, M. Itoh, N. Okita, and C. Jones Jr, *Energy Procedia* 37, 1135 (2013).
- V.T. Cheang, R.A. Hedderwick, and C. McGregor, *Sol. Energy* 113, 199 (2015).
- D.J. Young, *High Temperature Oxidation and Corrosion of Metals*, 2nd ed. (Oxford: Elsevier, 2016).
- D. Huenert and A. Kranzmann, *NACE Paper 08-447*, Houston, TX, presented at NACE Corrosion 2008, (New Orleans, LA, 2008).
- B.A. Pint and J.R. Keiser, *JOM* 67, 2615 (2015).
- B.A. Pint, R.G. Brese, and J.R. Keiser, *Mater. Corros.* 68, 151 (2017).
- B.A. Pint, R. Brese, and J.R. Keiser, *ASME Paper #GT2017-65066, for the International Gas Turbine & Aeroengine Congress & Exhibition* (Charlotte, NC, 2017).
- B.A. Pint, K.A. Unocic, R.G. Brese, and J.R. Keiser, *Mater. High Temp.* 35, 39 (2018).
- E.G. Feher, *Energy Convers.* 8, 85 (1968).
- H.E. McCoy, *Corrosion* 21, 84 (1965).
- W.R. Martin and J.R. Weir, *J. Nucl. Mater.* 16, 19 (1965).
- H.E. Evans, D.A. Hilton, and R.A. Holm, *Oxid. Met.* 10, 149 (1976).
- J.C.P. Garrett, J.T. Crook, S.K. Lister, P.J. Nolan, and J.A. Twelves, *Corros. Sci.* 22, 37 (1982).
- P.C. Rowlands, J.C.P. Garrett, L.A. Popple, A. Whittaker, and A. Hoaskey, *Nucl. Energy* 25, 267 (1986).
- Y. Gong, D.J. Young, P. Kontis, Y.L. Chiu, H. Larsson, A. Shin, J.M. Pearson, M.P. Moody, and R.C. Reed, *Acta Mater.* 130, 361 (2017).
- C.T. Fujii and R.A. Meussner, *J. Electrochem. Soc.* 114, 435 (1967).
- F. Rouillard, F. Charton, and G. Moine, *Corrosion* 67, 095001 (2011).
- T. Furukawa and F. Rouillard, *Prog. Nucl. Energy* 82, 136 (2015).
- R.I. Olivares, D.J. Young, P. Marvig, and W. Stein, *Oxid. Met.* 84, 585 (2015).
- R. Viswanathan, J.F. Henry, J. Tanzosh, G. Stanko, J. Shingledecker, B. Vitalis, and R. Purgert, *J. Mater. Eng. Perf.* 14, 281 (2005).
- G.C. Wood, I.G. Wright, T. Hodgkiess, and D.P. Whittle, *Werk. Korr.* 21, 900 (1970).
- G.H. Meier, W.C. Coons, and R.A. Perkins, *Oxid. Met.* 17, 235 (1982).
- B. Jönsson and C. Svedberg, *Mater. Sci. Forum* 251–254, 551 (1997).
- I.G. Wright and R.B. Dooley, *Int. Mater. Rev.* 55, 129 (2010).
- N. Mu, K.Y. Jung, N.M. Yanar, G.H. Meier, F.S. Pettit, and G.R. Holcomb, *Oxid. Met.* 78, 221 (2012).
- E. Essuman, L.R. Walker, P.J. Maziasz, and B.A. Pint, *Mater. Sci. Technol.* 29, 822 (2013).
- C.H. Oh, T. Lillo, W. Windes, T. Totemeier, B. Ward, R. Moore, and R. Barner, Idaho National Laboratory Report INL/EXT-06-01271, (2006).
- H.J. Lee, H. Kim, S.H. Kim, and C. Jang, *Corros. Sci.* 99, 227 (2015).
- J. Mahaffey, D. Adam, A. Brittan, M. Anderson, and K. Sridharan, *Oxid. Met.* 86, 567 (2016).
- L.M. Pike, in *Superalloys 2008*, eds. by R.C. Reed et al. TMS (Warrendale, PA, 2008), p. 191.
- A. Chyrkin, P. Huczukowski, V. Shemet, L. Singheiser, and W.J. Quadackers, *Oxid. Met.* 75, 143 (2011).
- M.J. Lance and B.A. Pint, in *Proceedings of the 6th International Symposium on Supercritical CO₂ Power Cycles* (Pittsburgh, PA, 2018), Paper #117 (2018).
- B.A. Pint and K.A. Unocic, *Oxid. Met.* 87, 515 (2017).
- Z. Zeng, K. Natesan, Z. Cai, and S.B. Darling, *Nat. Mater.* 7, 641 (2008).
- D.J. Young, T.D. Nguyen, P. Felfer, J. Zhang, and J.M. Cairney, *Scripta Mater.* 77, 29 (2014).
- I. Wolf and H.J. Grabke, *Solid State Commun.* 54, 5 (1985).
- T.D. Nguyen, J. Zhang, and D.J. Young, *Corr. Sci.* 76, 231 (2013).
- W.J. Quadackers, H. Holzbrecher, K.G. Briefs, and H. Beske, *Oxid. Met.* 32, 67 (1989).